Corneal epithelial healing after photorefractive keratectomy: Analytical study

Sebastiano Serrao, MD, PhD, Marco Lombardo, MD

Purpose: To characterize the velocity of epithelial migration after photorefractive keratectomy (PRK) with 3 different corneal ablation patterns.

Setting: Department of Ophthalmology, Catholic University of Rome, Rome, Italy.

Methods: Fifteen patients (30 eyes) with mild to moderate myopia and with simple to compound myopic astigmatism were enrolled for this study. The surgical procedure consisted of standardized PRK with final smoothing performed using the Technolas Keracor 217C excimer laser. The reepithelialization process was evaluated at 0 hours, 20 hours, 40 hours, and 60 hours after surgery using a digital photo camera and custom software for measurement. Digital analysis of the images was performed. Corneal topographies were taken at 1 month, 3 months, 6 months, and 12 months after PRK.

Results: The mean speed of radial migration in the 10 eyes (33%) in the low spherical ablation group was 0.087 mm/h ± 0.008 (SD). This was significantly higher than that found in the 10 eyes (33%) in the high spherical ablation group (mean speed 0.078 ± 0.007 mm/h; $P < .001$) and in the 10 eyes (33%) in the cross-cylinder ablation group (mean speed 0.055 ± 0.014 mm/h; $P < .001$).

Conclusion: Analysis of the data shows that epithelial migration along the photoablated corneal surface depends on the ablation pattern. The epithelial sliding is highly influenced by local variations in the curvature of the stromal surface. The data demonstrate that faster epithelial wound healing after PRK is predictive of optimal visual performance.

J Cataract Refract Surg 2005; 31:930–937 © 2005 ASCRS and ESCRS

The epithelial renewal process after excimer laser refractive surgery involves 4 fundamental phases: cellular division, cellular migration, adhesion to the epithelial basal membrane, and epithelial–stromal interaction.[1–3] Hence, the rapid and correct reepithelialization of the cornea following surgery is essential for the maintenance of a high-quality visual acuity.

In the past few years, reepithelialization kinetics have been investigated in detail. Light microscope evaluations and immunohistochemistry analysis studies have shown that a large number of molecules are involved in this process.[4] Every corneal abrasion, with no damage to the Bowman's layer or stroma, heals in a symmetric fashion, indicating that the rate of cellular migration is equivalent at all points along the wound border.[5,6] In the renewal process, the epithelial cells are immediately able to establish appropriate connections with adjacent cells, maintaining the epithelial integrity and reducing the corneal surface's impermeability to external agents.[7] Thereafter, corneal epithelial cells secrete anchoring structures and basal membrane constituents that will come to complete organization once the epithelium has recovered its normal multistratified architecture.[8] Clinical and experimental studies[9–11] permit us to hypothesize that a smooth corneal surface and a tapered corneal profile are 2 very important variables for correct epithelial healing after

Accepted for publication August 27, 2004.

From Serraolaser (Serrao), Rome, Italy, and Department of Experimental and Clinical Medicine (Lombardo), University Magna Græcia of Cantanzaro, Cantanzaro, Italy.

No author has a financial or proprietary interest in any material or method mentioned.

Reprint requests to Sebastiano Serrao, MD, PhD, Via Orazio 31, 00193 Rome, Italy. E-mail: info@serraolaser.it.

0886-3350/05/$-see front matter
doi:10.1016/j.jcrs.2004.12.041

photorefractive keratectomy (PRK). Furthermore, rapid and noncomplicated epithelial healing has been correlated to the reduction in epithelial–stromal remodeling processes,[12] with less haze and refractive regression, allowing us to predict the refractive outcome and its stability more accurately.[13,14] A smoother anterior stromal ablated surface hastens epithelial adhesion and migration with faster epithelial wound closure than a more irregular ablated stromal bed.[10,15]

In a previous work, we analyzed how the smoothing technique accelerates epithelial wound repair after standard PRK.[9] The technique is similar to a phototherapeutic keratectomy (PTK)[16] and is used to obtain a smooth ablation surface thus eliminating gross and small irregularities and flattening the borders of the ablation edges. Smoothing is performed at the end of PRK, using a viscous solution with the optimal rheological properties.[17,18] As previously stated by others,[17,18] the ideal masking solution should have an ablation rate similar to that of corneal tissue (0.25 μm per pulse) and a viscosity that makes it cover the irregular surface uniformly without running off too quickly; in this manner, only the stromal peaks are left exposed. At present, the right solution for this purpose is a sodium hyaluronate 0.25%.[19]

In this work, we investigated the relationship between the epithelial healing dynamics and the differences in the regional curvature of the ablated corneas after PRK performed with 3 different ablation patterns.

Patients and Methods

Fifteen patients (9 women and 6 men) were enrolled in this study for a total of 30 eyes (100%). Sex was not considered a primary selection criterion.[20] The inclusion criteria were age between 22 and 52 years (mean 32.4 years ± 8.96 [SD]) and a manifest spherical equivalent refraction ranging from −1.50 to −9.00 diopters (D). The exclusion criteria were any systemic or ocular disease that could potentially interfere with the healing process of the cornea. Patients with lens opacities, glaucoma, uveitis, or keratoconus were excluded. Patients wearing contact lenses were asked to discontinue their use at least 4 weeks prior to the preoperative evaluation. The possible risks and complications were explained, and all patients gave their written informed consent.

Ten eyes (33%) (low spherical ablation group: 2 women and 3 men) had a spherical equivalent refraction (mean cycloplegic spherical equivalent) ± of −3.82 ± 0.60 D (mean cylinder −0.18 ± 0.31 D); 10 eyes (33%) (high spherical ablation group: 4 women and 1 man) had a spherical equivalent refraction of −6.61 ± 1.14 D (mean cylinder −0.28 ± 0.36 D); the remaining 10 eyes (33%) (cross-cylinder ablation group: 3 women and 2 men) had a spherical equivalent of −4.89 ± 2.25 D and a cylinder with the rule from −3.00 to −6.00 D. In the 2 spherical ablation groups, the cylinder component was no greater than 0.75 D.

The PRK procedure was performed using a Technolas Keracor 217C excimer laser (Bausch & Lomb Chiron Technolas) with a 6 mm ablation zone and a transition zone up to 9 mm; an active eye-tracker device was used. The astigmatism group was treated with a cross-cylinder technique[21]; hyperopic photorefractive astigmatism keratectomy (PARK) and myopic PARK were performed with a 6 mm ablation zone and a transition zone up to 9 mm.

Oxybuprocaine hydrochloride eyedrops (Novesina) were used for topical anesthesia. An Amoils brush was used to remove the corneal epithelium.

In all cases, PTK was performed at the end of the procedure using a viscous masking sodium hyaluronate 0.25% solution (smoothing technique) as previously described.[9]

Postoperatively, patients were prescribed micronomicin preservative-free eye drops (Luxomicina) 6 times daily until complete reepithelialization of the cornea, sodium diclofenac 0.1% preservative-free eye drops (Voltaren Ofta) 3 times daily for 3 days, topical fluorometholone 0.1% (Flarex) twice daily for 1 month after complete reepithelialization, and sodium hyaluronate 0.18% hypotonic solution preservative-free eye drops (Vismed) 5 times daily for 6 months after surgery. To avoid variability due to the mechanical effects of contact lenses, the patients were advised not to wear these devices.[22]

All eyes were comprehensively evaluated both preoperatively as well as postoperatively (on days 1, 2 and 3, after 1 week and after 1 month, 3 months, 6 months, and 12 months). Ocular evaluation included slitlamp biomicroscopy and the determination of the manifest and cycloplegic refraction, the uncorrected visual acuity, the spectacle-corrected visual acuity (BSCVA), and the corneal topography (Keratron Scout; Optikon 2000). Noncontact tonometry, ultrasonic pachymetry, and indirect ophthalmoscopy were also performed.

A series of digital photographs (Nikon Coolpix 995 Digital Camera, 3.40 megapixels) of the fluorescein-stained corneas was taken 0 hours, 20 hours, 40 hours, and 60 hours after surgery. Each photograph was taken twice to ensure the accuracy of the measures. Photographs taken 0 hours and 60 hours after surgery were not considered because of the nonlinear reepithelialization rate during these phases.[5,7]

Digital analysis was performed on the images (Figures 1, *a* and 1, *b*): Detection of the epithelial leading edge

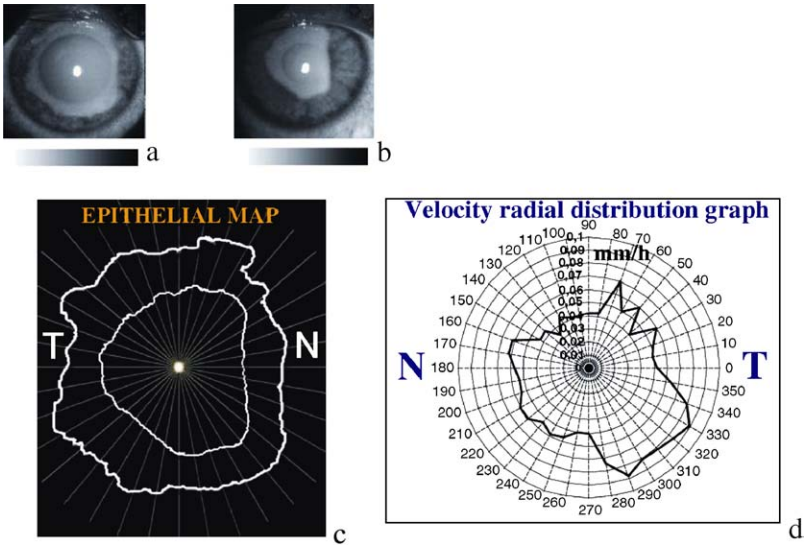

Figure 1. A right eye of the cross-cylinder ablation group. *a*: The green channel of the RGB standardized photograph of the fluorescein-stained cornea shows, 20 hours following surgery, the ablated stroma without the epithelial layer. *b*: The same cornea 40 hours from surgery. *c*: The epithelial leading edge after surgery respectively at the 40th hour (internal white line) and at the 20th hour (external with line) obtained by digital analysis processing of photographs *a* and *b*. *d*: Graph of the output of the model customized in to calculate the epithelial migration velocity distribution after surgery for 36 corneal meridians.

(Figure 1, *c*) permitted drawing of an epithelial regrowth map (Figure 1, *d*) for each case in the study. Figure 1, *d* shows the radial distribution of the epithelial migration velocity where the 0-degree was sited on the temporal side for every eye to compare the right to the left eye using the same criteria as those employed when evaluating the temporal/nasal asymmetry.

As suggested by other authors,[23] all the images were imported into custom-made software. This was done in order to place them in the same reference frame (the center of the reference frame was the center of the pupil) (Figure 2) and to convert the contours of the wound into numerical data. These data permitted calculation of the epithelial migration along the meridians centered on the pupil. The migration velocity was calculated as the ratio between the epithelial migration and the time interval between 2 sequential photographs.

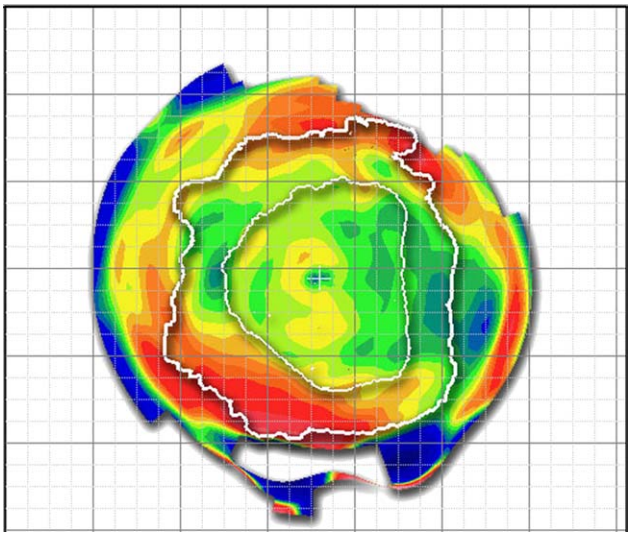

Figure 2. To correlate the reepithelialization kinetics to the regional variations in curvature, the same reference frame from the first month postoperative topography and the epithelial leading edge, centered on the pupil center, were imported. The figure shows a right eye in the cross-cylinder ablation group.

All the topographic tangential maps were considered as numerical output and imported into the same reference frame of the epithelial maps. They were evaluated using a new parameter: the differential circular profile. The Keratron topographer offers the possibility of displaying a group of data referred to a circular zone with a variable diameter on a graph. This tool allowed visualization of 2 groups of data referred to 2 circles in the same graph. Two circles with a diameter of 6 mm and 3 mm and the pupil as center were chosen to understand the difference in curvature that the progressing epithelium meets between 20 and 40 hours after PRK. Previous study showed that the epithelial edge migrates along this corneal region during this time.[9]

The best-fit topographic irregularity index (BFTi), described by Maloney and coauthors,[24] was used to analyze the first corneal surface smoothness both preoperatively as well as during follow-up.

Statistics

Two-way analysis of variance was used to compare the epithelial migration velocity to the different ablation corneal profiles. Paired Student *t* test was used to compare the 1-year postoperative and preoperative BFTi values. *P* values $<.05$ were considered statistically significant.

Results

Different ablation corneal profiles proved to significantly modify the epithelial migration speed between groups ($P<.001$). The mean speed of radial migration in the 10 eyes (33%) in the low spherical

ablation group was 0.087 ± 0.008 mm/h. This was significantly higher than that found in the 10 eyes (33%) in the high spherical ablation group (0.078 ± 0.007 mm/h; $P<.001$) and in the 10 eyes (33%) in the cross-cylinder ablation group (0.055 ± 0.014 mm/h; $P<.001$).

Table 1 and Figure 3 show, for all cases in the study, the mean progression of migration for each of the following corneal quadrants: 50 to 130 degrees, 140 to 220 degrees, 230 to 310 degrees, 320 to 40 degrees. One may readily note the differences in epithelial migration between the quadrants. These differences were less consistent in the low spherical ablation group.

Figure 4 shows the mean of the circular differential profiles in the 3 study groups. The differences in curvature between 6 mm and 3 mm from the center of the pupil were higher in the high spherical ablation group than in the low spherical ablation group. This is not surprising given the deeper laser ablation. The cross-cylinder ablation group showed a negative difference in the corneal horizontal meridians (0 to 180 degrees), which corresponds to the hyperopic ablation pattern for the correction of the with-the-rule astigmatism. Thereafter, the variation in the curvature values between the corneal quadrants was smaller in the 2 spherical ablation groups than in the astigmatic group. Figure 5 shows the circular differential profiles (CDP) between 6 mm and 3 mm for 3 eyes, 1 in each of the 3 study groups. In the cross-cylinder ablation group, the distribution of the curvature along the meridians was not homogeneous; in particular, at 6 mm the correction of the astigmatism was less consistent than with the 3 mm circle. In the other 2 groups, the variation in curvature along the meridians between 6 mm and 3 mm was homogeneous,

Table 1. Mean radial epithelial migration velocity for each corneal quadrant in the high and low spherical ablation groups and in the cross-cylinder ablation group.

Quadrant	Low Spherical Ablation Group	High Spherical Ablation Group	Cross-cylinder Ablation Group
40°–320° Temporal quadrant	0.097 ± 0.009	0.082 ± 0.006	0.067 ± 0.010
50°–130° Superior quadrant	0.078 ± 0.009	0.075 ± 0.010	0.041 ± 0.010
140°–220° Nasal quadrant	0.087 ± 0.008	0.076 ± 0.007	0.060 ± 0.022
230°–310° Inferior quadrant	0.086 ± 0.007	0.081 ± 0.006	0.054 ± 0.016

Mean ± SD

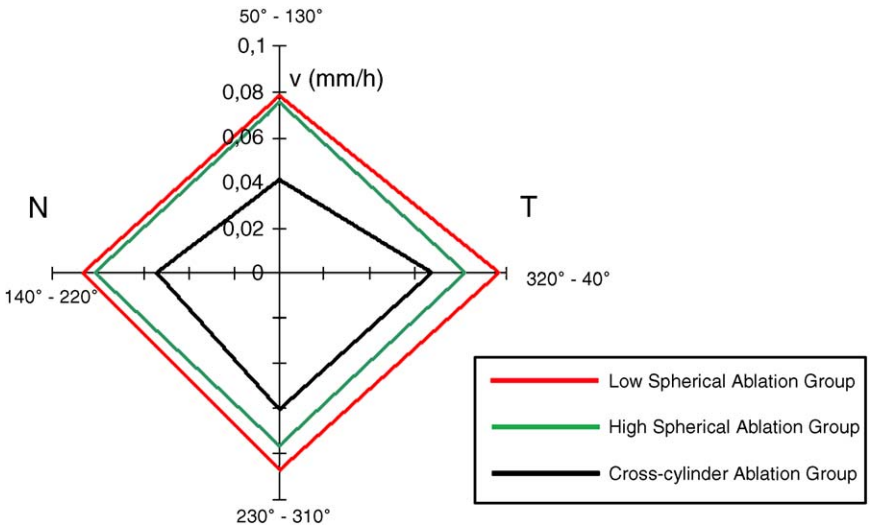

Figure 3. The mean radial epithelial migration velocity in the 3 study groups. The zero degrees was sited on the temporal side for every eye. This was done to compare the right to the left eye using the same criteria as those employed when evaluating the temporal/nasal asymmetry. The 2 spherical ablation groups show homogeneous epithelial migration along all the corneal meridians, whereas the cross-cylinder group shows faster epithelial healing in the temporal quadrant.

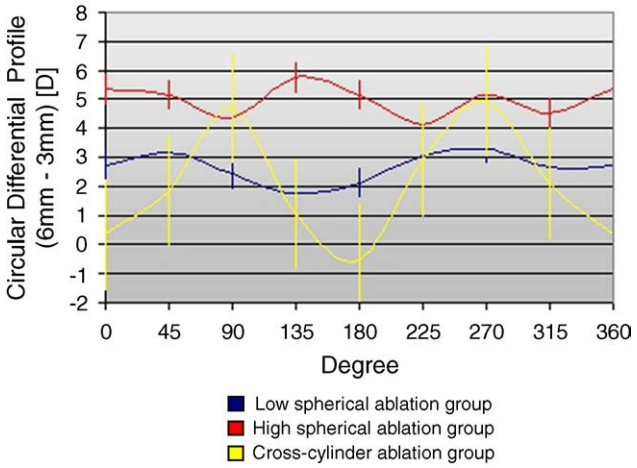

Figure 4. The mean circular differential profile of the 3 study groups. The *y*-axis represents the difference in diopters between 2 circular zones of the ablated corneal surface: The outer zone is 6 mm from the center of the pupil, and the inner zone is 3 mm from the center of the pupil. The circular differential profile permits synthesis of the difference in local curvature encountered by the epithelial healing edge.

and was less in the low spherical ablation group than in the high spherical ablation group.

The 12-month follow-up data confirmed that all the procedures were safe (in no case were any Snellen lines of BSCVA lost) and effective, with a safety index of 1.11 in the low spherical ablation group, 0.9 in the high spherical ablation group and 1.00 in the cross-cylinder group. In the low spherical ablation group the efficacy index was 1.13 versus 1.06 in the high spherical ablation group, and 1.18 in the cross-cylinder group.[25] Table 2 summarizes the preoperative and the postoperative spherical equivalent refractions in the 3 study groups. The refractive target was emmetropia in all cases except 1 patient who requested monovision (a patient included in the cross-cylinder ablation group; refractive target in one eye: −1 D). At the end of follow-up, all the eyes (100%) in the low spherical group had a cycloplegic spherical equivalent refraction within ±0.50 D of emmetropia. In contrast, this result was achieved in 9 eyes (90%) of the high spherical group and in 4 eyes (40%) in the cross-cylinder group. Ten eyes (100%) in the high spherical group and 8 eyes (80%) in the cross-cylinder group were within ±1.00 D of emmetropia; in the cross-cylinder group all the eyes (100%) were within ±2.00 D of emmetropia.

Both the low spherical and cross-cylinder ablation groups showed a statistically significant decrease in the BFTi values after surgery ($P<.05$), whereas the high

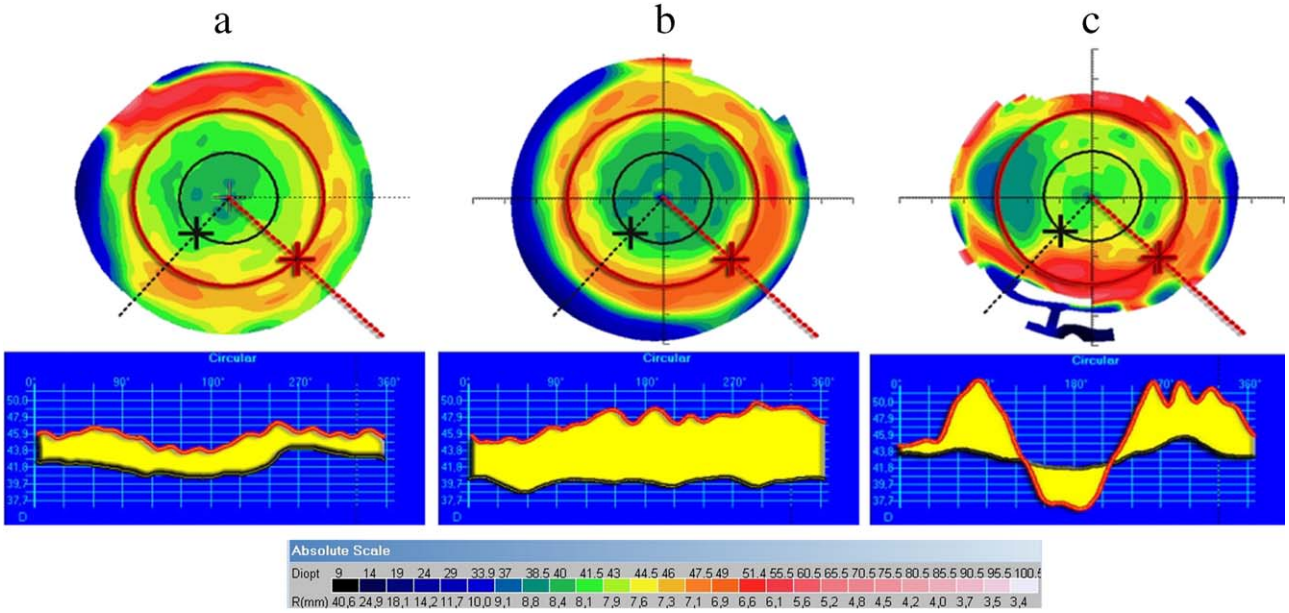

Figure 5. Between the 20th and 40th hours after PRK, the epithelium reached an area with a ray of curvature between 3 mm (black circle) and 6 mm (red circle) from the center of the reference frame of the imported images (pupil center). The CDP was created to allow analysis of the profile of this region. *a*: CDP of a low myopia case; the variation in curvature is low and homogeneous along the meridians. *b*: CDP of a high myopia case; the variation in curvature is high and homogeneous along the meridians. *c*: CDP of a cross-cylinder case; the variation in curvature is high and inhomogeneous along the meridians.

Table 2. Cycloplegic spherical equivalent refraction (Mean ± SD) during follow-up in the 3 study groups.

Patient Group	Preoperative (D)	3 months (D)	6 months (D)	12 months (D)
Low spherical ablation	−3.82 ± 0.60	+0.18 ± 0.21	+0.10 ± 0.37	−0.06 ± 0.20
High spherical ablation	−6.61 ± 1.14	+0.43 ± 0.66	+0.23 ± 0.53	+0.14 ± 0.29
Cross-cylinder ablation	−4.89 ± 2.25	−0.85 ± 0.78	−0.77 ± 0.48	−0.77 ± 0.48

spherical ablation group showed a significant increase in the BFTi values induced by surgery ($P<.05$): hence, the preoperative and 12-month postoperative corneal regularity indexes were, respectively, 0.34 and 0.30 in the low spherical group, 0.38 and 0.54 in the high spherical group, and 0.37 and 0.34 in the cross-cylinder group (Figure 6).

Discussion

Excimer laser corneal ablation gives rise to epithelial-stromal remodeling.[26,27] The variability in the outcome of corneal refractive surgery largely depends on the biophysical response of the corneal tissue.[28] This phenomenon contributes to refractive regression and corneal haze.[29,30] Many factors may influence corneal surface remodeling: the surgical technique itself,[31–33] the excimer laser systems,[34–38] and ocular movements. All these factors result in a quite irregular ablated surface, delayed epithelial healing, and altered stromal remodeling.[39,40] Thereafter, rapid epithelial wound closure is necessary for an optimal recovery of the corneal surface.[13,41]

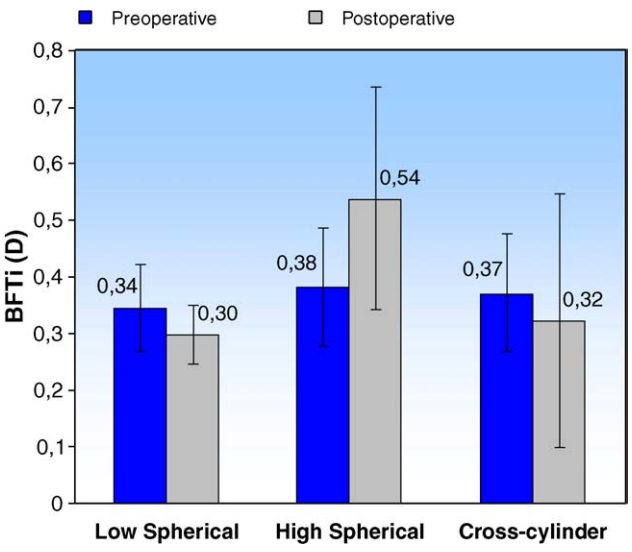

Figure 6. Corneal regularity index (BFTi) 12 months after surgery in the 3 study groups. After surgery, the high spherical ablation group had more irregularity of the central corneal surface than the other 2 study groups. The bars represent the standard deviation.

In this work, we evaluated epithelial regeneration on the postmyopic PRK corneal surface. Some variables were not taken into consideration owing to the different corneal profiles and the physiopathologic activity of the anterior stroma.[16,41,42] Instead, we focused our attention on the wound area, on the time necessary for healing, and on a new operative variable: the ablation pattern. Other authors have previously reported a correlation between the corneal map and epithelial renewal.[43]

We observed that 30 hours following surgery, the epithelial edge may be localized within the 4 central millimeters of the cornea.[9] We simplified the migration dynamics by using a linear mathematical model. At the same time, we also evaluated the Maloney index (BFTi), which is a topographic regularity index over a 4 mm central corneal surface.

We defined the CDP as the variation in curvature along the topographic meridians. We demonstrated that the greater this variation, the slower the epithelial migration along the corneal surface.

Our study results showed a significantly slower progression of the epithelium in the higher spherical and cross-cylinder ablation groups than in the low spherical ablation group, probably due to a more rapid and steeper change of the corneal profile in the ablation zone. Thereafter, the high spherical ablation group showed significantly faster epithelial migration than that observed in the cross-cylinder ablation group. On the other hand, and in contrast to the high spherical ablation group, the cross-cylinder ablation group showed a significant increase in the regularity of the postoperative central first corneal surface as expressed by BFTi analysis. The significance of this observation is that laser ablation effectively reduces the 4 mm central cornea toricity. Nevertheless, the Maloney index does not account for the medium corneal periphery where, as

shown at circular topographic profilometry analysis, an increase in the curvature asymmetry after a cross-cylinder procedure has been found. The marked asymmetry of the stromal bed in the medium corneal periphery may explain the lesser migration of the epithelial edge in astigmatic ablation as compared with spherical ablation. It would be useful to define a new topographic index that accounts even for the variation in curvature of the medium corneal periphery.

A decrease in the BFTi value after surgery correlates with less induced high-order optical aberrations and with a high-quality visual performance.[13] In this work, the low spherical ablation group showed a higher predictability of the targeted refractive outcome than that observed in the 2 other study groups. However, we are aware that, besides slowing epithelial healing, a more irregular and a less tapered ablated corneal surface intensifies the stromal remodeling process,[26,40] thus reducing the predictability of the refractive outcome when PRK is performed in patients with high spherical and astigmatic myopia.

The PTK-style treatment after PRK proved to be a safe procedure,[9,13] the main complication being the induction of a slight hyperopic shift of the attempted correction when using a masking fluid and setting a low ablation depth with a large ablation zone and transition zones.[44]

In conclusion, we demonstrated that following excimer laser ablation, the corneal epithelium does not heal in a symmetric manner and that epithelial migration is strongly dependent on local variations in the curvature of the postoperative corneal surface.

Hence, a postoperative smooth stromal surface and a more regular ablation profile are necessary to achieve an optimal surgical outcome after PRK.

References

1. Ren H, Wilson G. The cell shedding rate of the corneal epithelium—a comparison of collection methods. Curr Eye Res 1996; 15:1054–1059
2. Daniels JT, Dart JKG, Tuft SJ, Khaw PT. Corneal stem cells in review. Wound Repair Regen 2001; 9:483–494
3. Gaffney EA, Maini PK, Sherratt JA, Tuft S. The mathematical modelling of cell kinetics in corneal epithelial wound healing. J Theor Biol 1999; 197:15–40
4. Zagon IS, Sassani JW, McLaughlin PJ. Reepithelialization of the human cornea is regulated by endogenous opioids. Invest Ophthalmol Vis Sci 2000; 41:73–81
5. Crosson CE, Klyce SD, Beuerman RW. Epithelial wound closure in the rabbit cornea; a biphasic process. Invest Ophthalmol Vis Sci 1986; 27:464–473
6. Estil S, Kravik K, Haaskjold E, et al. Pilot study on the time course of apoptosis in the regenerating corneal epithelium. Acta Ophthalmol Scand 2002; 80:517–523
7. Lu L, Reinach PS, Kao WW-Y. Corneal epithelial wound healing. Exp Biol Med 2001; 226:653–664
8. Gipson IK, Spurr-Michaud S, Tisdale A, Keough M. Reassembly of the anchoring structures of the corneal epithelium during wound repair in the rabbit. Invest Ophthalmol Vis Sci 1989; 30:425–434
9. Serrao S, Lombardo M, Mondini F. Photorefractive keratectomy with and without smoothing: a bilateral study. J Refract Surg 2003; 19:58–64
10. Lombardo M, Serrao S. Smoothing of the ablated porcine anterior corneal surface using the Technolas Keracon 217C and Nidek EC-5000 excimer lasers. J Refract Surg 2004; 20:450–453
11. Horgan SE, McLaughlin-Borlace L, Stevens JD, Munro PMG. Phototherapeutic smoothing as an adjunct to photorefractive keratectomy in porcine corneas. J Refract Surg 1999; 15:331–333
12. Møller-Pedersen T, Vogel M, Li HF, et al. Quantification of stromal thinning, epithelial thickness, and corneal haze after photorefractive keratectomy using in vivo confocal microscopy. Ophthalmology 1997; 104:360–368
13. Serrao S, Lombardo M. One-year results of photorefractive keratectomy with and without surface smoothing using the Technolas 217C laser. J Refract Surg 2004; 20:444–449
14. Detorakis ET, Siganos DS, Kozobolis VP, Pallikaris IG. Corneal epithelial wound healing after excimer laser photorefractive and photoastigmatic keratectomy (PRK and PARK). Cornea 1999; 18:25–28
15. Steele JG, Johnson G, McLean KM, et al. Effect of porosity and surface hydrophilicity on migration of epithelial tissue over synthetic polymer. J Biomed Mater Res 2000; 50:475–482
16. Dogru M, Katakami C, Miyashita M, et al. Ocular surface changes after excimer laser phototherapeutic keratectomy. Ophthalmology 2000; 107:1144–1152
17. Kornmehl EW, Steinert RF, Puliafito CA. A comparative study of masking fluids for excimer laser phototherapeutic keratectomy. Arch Ophthalmol 1991; 109:860–863
18. Keates RH, Bloom RT, Schneider RT, et al. Absorption of 308-nm excimer laser radiation by balanced salt solution, sodium hyaluronate, and human cadaver eyes. Arch Ophthalmol 1990; 108:1611–1613
19. Tadmor R, Chen N, Israelachvili JN. Thin film rheology and lubricity of hyaluronic acid solutions at a normal

physiological concentration. J Biomed Mater Res 2002; 61:514–523
20. Goto T, Klyce SD, Zheng X, et al. Gender- and age-related differences in corneal topography. Cornea 2001; 20:270–276
21. Vinciguerra P, Sborgia M, Epstein D, et al. Photorefractive keratectomy to correct myopic or hyperopic astigmatism with a cross-cylinder ablation. J Refract Surg 1999; 15:S183–S185
22. O'Leary DJ, Madgewick R, Wallace J, Ang J. Size and number of epithelial cells washed from the cornea after contact lens wear. Optom Vis Sci 1998; 75:692–696
23. Mahmoud AM, Roberts C, Herderick EE. The Ohio State University Corneal Topography Tool. ARVO abstract 3599. Invest Ophthalmol Vis Sci 2000; 41(4):S677
24. Maloney RK, Bogan SJ, Waring GO III. Determination of corneal image-forming properties from corneal topography. Am J Ophthalmol 1993; 115:31–41
25. Koch DD, Kohnen T, Obstbaum SA, Rosen ES. Format for reporting refractive surgical data [editorial]. J Cataract Refract Surg 1998; 24:285–287
26. Wilson SE, Mohan RR, Hong J-W, et al. The wound healing response after laser in situ keratomileusis and photorefractive keratectomy; elusive control of biological variability and effect on custom laser vision correction. Arch Ophthalmol 2001; 119:889–896
27. Gan L, Hamberg-Nyström H, Fagerholm P, Van Setten G. Cellular proliferation and leukocyte infiltration in the rabbit cornea after photorefractive keratectomy. Acta Ophthalmol Scand 2001; 79:488–492
28. Baldwin HC, Marshall J. Growth factors in corneal wound healing following refractive surgery: a review. Acta Ophthalmol Scand 2002; 80:238–247
29. Fantes FE, Hanna KD, Waring GO III, et al. Wound healing after excimer laser keratomileusis (photorefractive keratectomy) in monkeys. Arch Ophthalmol 1990; 108:665–675
30. Jester JV, Møller-Pedersen T, Huang J. The cellular basis of corneal transparency: evidence for ''corneal crystallins.'' J Cell Sci 1999; 112:613–622
31. Weiss RA, Liaw L-HL, Berns M, Amoils SP. Scanning electron microscopy comparison of corneal epithelial removal techniques before photorefractive keratectomy. J Cataract Refract Surg 1999; 25:1093–1096
32. Fasano AP, Moreira H, McDonnell PJ, Sinbawy A. Excimer laser smoothing of a reproducible model of anterior corneal surface irregularity. Ophthalmology 1991; 98:1782–1785
33. Vinciguerra P, Azzolini M, Airaghi P, et al. Effect of decreasing surface and interface irregularities after photorefractive keratectomy and laser in situ keratomileusis on optical and functional outcomes. J Refract Surg 1998; 14:S199–S203
34. Fiore T, Carones F, Brancato R. Broad beam vs. flying spot excimer laser: refractive and videokeratographic outcomes of two different ablation profiles after photorefractive keratectomy. J Refract Surg 2001; 17:534–541
35. Liang F-Q, Ishikawa T, Kim J, et al. Surface quality of excimer laser corneal ablation with different frequencies. Cornea 1993; 12:500–506
36. Fantes FE, Waring GO III. Effect of excimer laser radiant exposure on uniformity of ablated corneal surface. Lasers Surg Med 1989; 9:533–542
37. Huang D, Arif M. Spot size and quality of scanning laser correction of higher-order wavefront aberrations. J Cataract Refract Surg 2002; 28:407–416
38. Bleckmann H, Schnoy N, Kresse H. Electron microscopic and immunohistochemical examination of scarred human cornea re-treated by excimer laser. Graefes Arch Clin Exp Ophthalmol 2002; 240:271–278
39. Taylor SM, Fields CR, Barker FM, Sanzo J. Effect of depth upon the smoothness of excimer laser corneal ablation. Optom Vis Sci 1994; 71:104–108
40. Møller-Pedersen T, Cavanagh HD, Petroll WM, Jester JV. Stromal wound healing explains refractive instability and haze development after photorefractive keratectomy; a 1-year confocal microscopic study. Ophthalmology 2000; 107:1235–1245
41. Wilson SE. Molecular cell biology for the refractive corneal surgeon: programmed cell death and wound healing. J Refract Surg 1997; 13:171–175
42. Moller-Pedersen T, Li HF, Petroll WM, et al. Confocal microscopic characterization of wound repair after photorefractive keratectomy. Invest Ophthalmol Vis Sci 1998; 39:487–501
43. Grimm B, Waring GO III, Ibrahim O. Regional variation in corneal topography and wound healing following photorefractive keratectomy. J Refract Surg 1995; 11: 348–357
44. Dogru M, Katakami C, Yamanaka A. Refractive changes after excimer laser phototherapeutic keratectomy. J Cataract Refract Surg 2001; 27:686–692